THERMOSET COMPOSITE ASSEMBLING METHOD BY WELDING OF THERMOPLASTIC SURFACE LAYERS: MICROSTRUCTURE AND TOUGHNESS OF THE RESULTING THERMOPLASTIC/EPOXY RESIN INTERFACES.

Q. Voleppe[a*], T. Pardoen[b], C. Bailly[a]

[a]*Institute of Condensed Matter and Nanosciences (IMCN), Department of Bio and soft matter (BSMA), Université catholique de Louvain, Croix du Sud 1, 1348 Louvain-la-Neuve.*
[b]*Institute of Mechanics, Materials and Civil Engineering (iMMC), Department of Materials and process engineering (IMAP), Université catholique de Louvain, Croix du Sud 1, 1348 Louvain-la-Neuve.*
**quentin.voleppe@uclouvain.be*

Keywords: thermoplastic, thermoset, interface, toughness.

Abstract

The morphology, composition gradient and fracture toughness of thermoplastic/thermoset interfaces based on the RTM6 epoxy resin and on either poly(ether sulfone) or poly(ether imide) are studied as a function of the curing cycle. The microstructure gradients observed by optical microscopy are characterized by a narrow interface only presenting sea-island morphologies in the case of poly(ether sulfone) while a co-continuous region is obtained at the interface when poly(ether imide) is considered. This better compatibility between poly(ether imide) and RTM6 is also highlighted by higher interdiffusion lengths, giving the poly(ether imide)/RTM6 interface cracks higher initiation toughness values. The observation of fracture surfaces confirm this result, showing clear crack meandering paths in the case of poly(ether imide).which are not observable when poly(ether sulfone) is considered.

Introduction

In the context of the necessity for the aeronautical field to improve the joining methods dedicated to the assembling of composites parts, a promising alternative to mechanical fastening methods called Thermoset Composite Welding (TCW) has received growing interest in recent years [1]. This method (Figure 1) consists in thermally welding two thermoset composite parts together by partial fusion (step 2) of two thermoplastic layers previously placed at their surface during a preliminary co-curing step (step 1). One of the key aspects to be considered in TCW is the damage resistance of the thermoplastic/thermoset interfaces involved in the formation of the joint and generated during this preliminary co-curing step. More specifically, an in-depth understanding of the relationships between the complex microstructure gradient in the interdiffusion zone and the corresponding damage mechanisms would definitely lead to the improvement of the quality of the welds.

In this context, the present paper aims at exposing the results obtained for various thermoplastic/thermoset interfaces studied as a function of the curing cycle and the thermoplastic considered. To this end, five major points are discussed: the choice of the

materials as well as the definition of the curing cycles and of the model samples, the determination of the concentration profiles in the interdiffusion zone, the characterization of the morphology gradient generated at the interface, the measurements of the corresponding initiation toughness and finally the observation of fracture surfaces from broken SENB specimens.

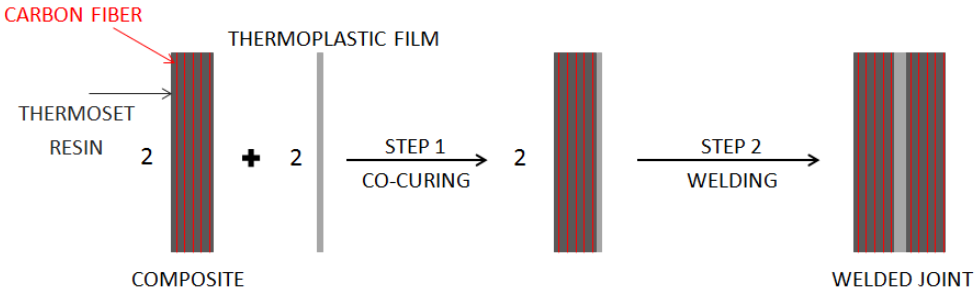

Figure 1. Schematic view of the thermoset composite welding process: the first step consists in co-curing the un-cured thermoset composite with a thermoplastic layer at its surface. The second step is the thermoplastic welding of two co-cured parts by partial fusion of the thermoplastic layers.

1. Choice of the materials, definition of the curing cycles and preparation of the samples

The research is performed on model systems based on the mono-component RTM6 epoxy resin produced by Hexcel and certified for aeronautical applications and on thermoplastic layers made of high performance polymers also used in aeronautics: either poly(ether sulfone) (PES) from Solvay or poly(ether imide) (PEI) from Sabic. Several layer thicknesses were used, such as 200, 100, 50 or even 30 µm. The interest using these polymers is that they have similar values of T_g as cured RTM6, being around 220°C.

Different temperature cycles were also applied to cure the thermoplastic/thermoset interfaces. The four cycles considered in this document are represented in Figure 2.

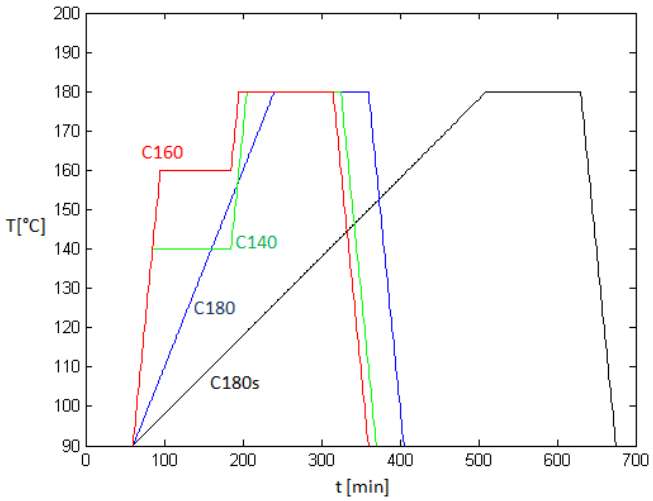

Figure 2. Definition of the four curing cycles considered in this document. The C_{160} and the C_{140} cycles are defined by heating ramps of 2°C/min and an intermediate plateau at 160°C during 90 minutes and at 140°C during 100 minutes respectively. The C_{180} and C_{180s} cycles are characterized by a heating ramp of 0.5°C/min and 0.2°C/min respectively and by no intermediate plateau. All 4 cycles have a post-curing plateau at 180°C during 120 minutes followed by an ending cooling ramp.

The model systems prepared for this study (Figure 3) consist in sandwich structures made of one single thermoplastic layer surrounded at each side by RTM6 resin. The thermoplastic layer is initially put in contact with the uncured resin in a metallic mold coated with a demolding agent. The structure is then co-cured by applying one of the temperature cycle presented in Figure 2. As a consequence of this preparation procedure, the sandwich samples are characterized by the absence of carbon fibers in the thermoset. The welding step described previously is also avoided since there is no thermoplastic/thermoplastic interface to consider. It is then possible to exclusively focus on the processes taking place during the co-curing step in the interfacial zone: the interdiffusion of both thermoplastic molecules and RTM6 reactive species through the initially sharp interface, the increase in molecular weight of the RTM6 resin upon curing leading eventually to gelation of the system and the phase separation process resulting from the interaction between the two latter phenomena.

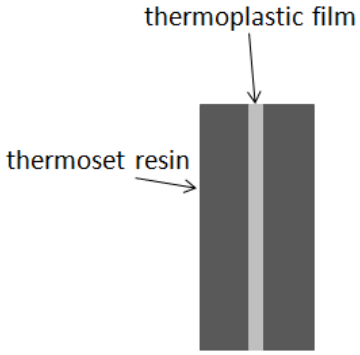

Figure 3. Schematic view of the model systems considered in this study. No carbon fiber and no thermoplastic/ thermoplastic interface are present in this type of simplified system, the focus being put on the thermoplastic/ thermoset interfaces.

2. Determination of the concentration profiles along the interdiffusion zone

The concentration profiles of interfaces based on PES were determined by means of Raman spectroscopy coupled to chemometrics. The spectra of pure PES and pure RTM6 as well as homogeneous blends of intermediate compositions were recorded in order to develop a chemometric model. This model was then applied to model samples in order to predict the evolution of the composition along the interface.

The concentration profiles obtained by applying the C_{160}, C_{140} and C_{180} curing cycles to different samples of same PES thickness show that the shortest interdiffusion length was obtained with the cycle having the longest gel time, i.e. the C_{180} cycle, with a value around 35 µm. Conversely, the longest interdiffusion length was observed in samples cured following the cycle of shortest gel time, i.e. the C_{160} cycle, with a value around 70 µm. This result suggests that, for the operating window investigated in this study, the interdiffusion kinetics, mainly ruled by temperature, is predominant over the RTM6 curing kinetics.

The comparison between the profiles obtained for a given curing cycle but with different film thicknesses also showed that it was possible to modify the shape of the concentration profile

below a certain critical thickness, depending on the curing cycle applied. Above this critical thickness, the center of the sample still contains pure, un-swollen PES and the shape of the interdiffusion zone remains unchanged whatever the initial thickness of the thermoplastic layer. Below this threshold, no zone of pure PES is observable and the thermoplastic content at the center of the sample decreases as the initial layer thickness decreases.

The interdiffusion lengths for PEI/RTM6 interfaces could not be determined using Raman spectroscopy as no clear characteristic peak in the respective spectra of the pure materials was observable in order to distinguish them. However, an analysis of several images from optical microscopy highlighted an enhanced compatibility between PEI and the RTM6 reactive species compared to the PES-RTM6 couple. Indeed, for a given curing cycle the interfaces based on PEI presented longer interdiffusion lengths than the samples based on PES.

3. Characterization of the morphology gradients

As briefly mentioned previously, the microstructural characterization of the interdiffusion zone was performed for the different curing cycles on both PES and PEI based samples using optical microscopy. Both for PES and PEI based interfaces a nodular dispersion of RTM6 in thermoplastic-rich zones as well as the phase inverted morphology in RTM6-rich zones were observable. In the case of PES/RTM6 interfaces, no consequent change in microstructure gradient in function of the curing cycle was observed, the C_{160}, C_{140} and C_{180} cycles giving similar morphology gradients. Moreover, no co-continuous phase was present at the thermoplastic/thermoset interface, the transition between the two nodular morphologies being very sharp.

In the case of PEI based interfaces, the changes in the microstructure gradient in function of the curing cycle were more visible and could be highlighted using the very slow heating rate C_{180s} cycle giving a sharp interface without swelling of the thermoplastic film by the RTM6 reactive species. When considering the 3 first cycles, the microstructure gradients were quite similar to what Lestriez et al. observed in interfaces composed of PEI and an epoxy resin [2]. The presence of a co-continuous phase making a smooth transition between the two nodular morphologies as well as the finer RTM6 nodular dispersion into PEI-rich zones compared to the one observed into PES-rich zones also confirm the higher compatibility between PEI and RTM6 than PES and RTM6.

4. Cracking initiation toughness measurements

SENB measurements were performed in order to obtain information about the fracture toughness of the interfaces. The tests were carried on according to the ASTM D5045-99. The pre-crack was not generated using a razor blade but was initially present thanks to the insertion of a 30 µm thick poly(imide) film at the initial thermoplastic/RTM6 interface before the co-curing, as illustrated in Figure 4.

A comparison between the PES/RTM6 and PEI/RTM6 interfaces at given curing cycle and film thickness was performed, as well as the influence of the curing cycle on the toughness of PEI/RTM6 interfaces. The results show that the cracking initiation toughness related to the PEI/RTM6 interfaces is approximately 5 times higher than the value for pure RTM6 and 2 times higher than for PES/RTM6 interfaces. This result is in accordance with the fact that longer interdiffusion lengths, better compatibility and the presence of a co-continuous phase between the two nodular phases in the morphology gradients are known to have a favorable influence on the toughness of the interfaces [3,4]. It also suggests that the damage mechanisms taking place in the interfaces are quite different when switching from PES to PEI. SEM observations of the fracture surfaces from the broken SENB specimen described in point 5 below confirm this supposition.

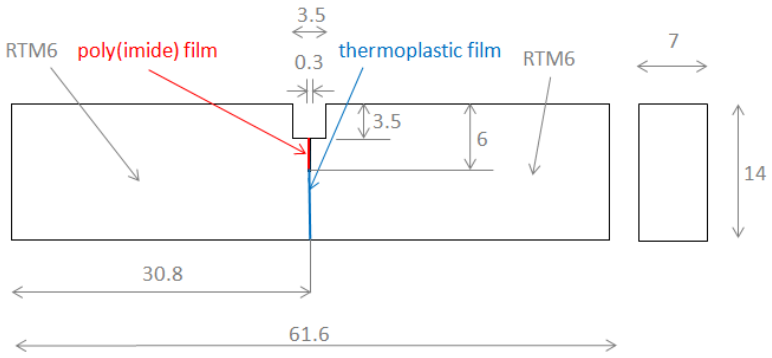

Figure 4. Representation of the SENB specimens with a poly(imide) film inserted between the thermoplastic film and the RTM6 resin before the co-curing in order to initiate the crack during the test.

The comparison between the PEI/RTM6 interfaces for the same film thickness but at different curing cycles showed that major differences in fracture toughness could be obtained as soon as two distinct cycles led to very dissimilar morphology gradients. For instance, the initiation toughness associated to the C_{160} cycle was almost 2 times higher than the value corresponding to the C_{180s} cycle which dropped to similar values than in the PES/RTM6 interfaces. On the other hand, when using two curing cycles giving rise to similar morphology gradients, the initiation toughness of the corresponding PEI/RTM6 interfaces were of the same order of magnitude. For instance, PEI/RTM6 samples curing following the C_{180} and C_{160} cycles presented very similar microstructure gradients in the interdiffusion zone and described above. They consequently were characterized by very close values of the initiation toughness.

5. Characterization of the fracture surfaces

The fracture surfaces of the broken SENB specimens considered in section 4 were characterized via SEM observations. Two main results were evidenced.

No real characteristic pattern except river lines structures was observed on the PES/RTM6 fracture surfaces whatever the scale investigated, ranging from 1mm to 1µm. The surfaces were quite similar to those observed in pure RTM6 broken SENB specimens. In some regions however, a few nodules could be observed. From the description of the morphology gradient made in the previous points we can affirm that those nodules are composed of PES and are thus found in the RTM6 rich region of the interdiffusion zone. This result indicates that the crack mostly propagates either in the RTM6 rich zone of the PES/RTM6 interface or even

outside of the interface through pure RTM6 regions, explaining the low values of initiation toughness when PES is considered.

In the case of the PEI/RTM6 interfaces cured according to the C_{160} and C_{180} curing cycles, the fracture surfaces generally presented two distinct zones. In certain regions no characteristic pattern was observable, just like in the case of PES/RTM6 fracture surfaces, which is an indicator of the presence of the crack into pure RTM6. However, in other regions a crack meandering path composed of a succession of dark and light stripes was clearly visible. Those regions presented microstructural patterns similar to those observed by optical microscopy: nodular dispersions like in RTM6-rich zones were localized in the dark stripes while finer nodular dispersions like in PEI-rich zones were localized in the light stripes, with the microstructure situated at the separation between both dark and light stripes corresponding to the co-continuous zones of the optical microscopy images. These observations strongly suggest that once in the interdiffusion zone the crack is trapped in it and oscillates between the different regions, which increases its path through the material and as a consequence allows the PEI/RTM6 interfaces to dissipate more energy than the PES/RTM6 interfaces.

Conclusion

Several thermoplastic/RTM6 thermoset resin interfaces were characterized from a microstructural and mechanical point of view. The results associated to two different thermoplastic polymers, poly(ether sulfone) (PES) and poly(ether imide) (PEI), were compared as a function of the curing cycle. Both thermoplastics gave rise to morphology gradients made of a nodular dispersion of thermoset in thermoplastic-rich zones as well as the phase inverted morphology in thermoset-rich zones. However in the case of PES/RTM6 samples the interface was very sharp, with no co-continuous phase making the transition between the nodular dispersions, while PEI/RTM6 samples presented a diffuse interface characterized by the presence of a co-continuous layer giving a smooth transition between the nodular phases. Combined to a longer interdiffusion length in the case of PEI/RTM6 interfaces compared to their PES counterpart, these characteristics give the PEI/RTM6 interfaces values of initiation toughness 2 times higher. The SEM observations of the fracture surfaces from the broken SENB specimens are also in accordance with the previous results. No special pattern was visible on PES/RTM6 surfaces while for PEI/RTM6 interfaces crack meandering was clearly present, trapping the crack into the interdiffusion zone where it oscillates through the morphology gradient, increasing the length of its path and consequently improving the damage resistance of the interface.

However the exact damage mechanisms taking place in the interface and the precise role of the presence or absence of the co-continuous region into the morphology gradient have to be further investigated in order to go deeper into the understanding of those thermoplastic/thermoset interfaces.

The presence of the carbon fibers, which is known to have an influence on the interdiffusion on certain systems, comes naturally as the next step to be investigated into this study.

References

[1] M. Hou. Thermoplastic Adhesive for Thermoset Composites. In *Materials Science Forum*, volumes 706-709, pages 2968-2973, 2012.

[2] B. Lestriez, J-P Chapel, J-F Gérard. Gradient Interphase between Reactive Epoxy and Glassy Thermoplastic from Dissolution Process, Reaction Kinetics, and Phase Separation Thermodynamics. *Macromolecules*, 34:1204-1213, 2001.

[3] B. Lestriez, J. Duchet, J-P Chapel, J-F Gérard. In *European conference on Adhesion (EURHAD)*, pages 523-527, 2000.

[4] Y-S Kim, S-C Kim. Properties of Polyetherimide/Dicyanate Semi-interpenetrating Polymer Network Having the Morphology Spectrum. *Macromolecules*, 32:2334-2341, 1999.